JOURNAL OF SOLID STATE CHEMISTRY 117, 55–63 (1995)

Research on the $BaBiO_{3-\delta}$ System ($0 \leq \delta \leq 0.5$)

F. Abbattista, M. Vallino, A. Delmastro, D. Mazza, and S. Ronchetti

Dipartimento di Scienza dei Materiali e Ingegneria Chimica, Politecnico di Torino, 10129 Torino, Italy

Received December 5, 1994; accepted December 9, 1994

The reduction isobar T vs δ ($pO_2 = 0.21$ atm) of $BaBiO_{3-\delta}$ between 750 and 1050°C shows a trend with three near linear sections in the ranges 750–850°C, 850–1000°C, and 1000–1045°C, respectively. The quenching in liquid N_2 of first-section solids (phase I) does not prevent the transformations $Fm\bar{3}m \rightarrow R\bar{3} \rightarrow I2/m$ typical of the stoichiometric compound and their XRD patterns at room temperature are not different from that of the stoichiometric $BaBiO_3$. The quenching of the cubic structure $Pm\bar{3}m$ of solids in the second section (phase II) still originates a monoclinic structure, but one strongly perturbed by the high concentration of oxygen vacancies. As already pointed out by other authors, by neutron diffraction at high temperatures, the phase II to phase III transition (third section of the isobar) occurs, unusually, in a gradual way and it is nearly complete about the melting temperature (1045°C). The close resemblance of the XRD patterns of the terms of the Aurivillius series with those of $BaBiO_{2.56}$ (phase III) leads us to think that this last phase is the term limit of the above series. Its structure would therefore be characterized by a random distribution of Ba and Bi ions in the perovskite A and B sites. The reduction of $BaBiO_3$ in high purity N_2 ($pO_2 \approx 10^{-6}$ atm) yields the polymorphous solid $BaBiO_{2.50}$. At 1000°C it still shows a structure with the tetragonal symmetry of phase III. Between 1000 and 800°C this bright red solid shows a pseudocubic perovskite-type structure, while for lower temperatures it assumes a bright yellow color and a structure with monoclinic no-longer-perovskite-type symmetry. The equilibria between the solids of the examined system were also studied through annealing and quenching in water of solids with $\delta = 0.2$, 0.3, and 0.44, sealed in silica glass tubes. The results agree with the diagram already published by Beyerlein *et al.* (R. A. Beyerlein, A. J. Jacobson, and L. N. Yacullo, *Mater. Res. Bull.* 20, 877 (1985)) only for T values higher than 700°C. The eutectoid decomposition of phase II ($\delta = 0.2$) to phase I and phase III (at $T = 668 \pm 2$°C) and the subsequent decomposition of phase III to phase I plus the yellow phase $BaBiO_{2.5}$ (at 663 ± 2°C) disagrees, on the contrary, with the results of the above authors. The results of the simultaneous DTA, TG, and DTG analyses on the stoichiometric $BaBiO_3$ at $pO_2 = 0.21$ and 1 atm leads us to think that monophasic region II ($Pm\bar{3}m$) for adequate pO_2 ($pO_2 > 1$ atm) extends as far as the stoichiometric solid itself ($\delta = 0$).

1. INTRODUCTION

1.1. Preliminary Statements

Results of a crystallographic study on the various forms of $BaBi_3O_{5.5}$ were recently published (1). These forms are characterized by unusual perovskitic structures having cubic or pseudocubic body-centered elementary cell and disordered distribution of barium and bismuth ions in A and B sites.

Pursuing our research program on the $BaO–Bi_2O_3–O$ system, we began to inquire into solids with compositions ranging between the quoted polymorphous phase and $BaBiO_3$.

The first results clearly showed that the equilibria among the phases existing in this part of the system did not correspond with the perovskite-like solid solution as suggested by Saponov *et al.* (2), and that the understanding of those equilibria required an adequate knowledge of the various transformations that $BaBiO_3$ undergoes as the temperature changes.

1.2. Bibliographic Data

$BaBiO_3$ shows, at room temperature, a distorted perovskite lattice with monoclinic unit cell ($I2/m$) characterized by two different B sites, occupied respectively by Bi^{3+} and Bi^{5+} (3, 4).

At 132°C a first transition occurs, from monoclinic to rhombohedral ($R\bar{3}$); a second, from rhombohedral to cubic ($Fm\bar{3}m$), takes place at about 500°C. In these transitions both the stoichiometry and the ordered distribution of the Bi^{3+} and Bi^{5+} ions are preserved (3, 5, 6). These phase transitions are thoroughly reversible and it is not possible to cool the high temperature structures metastably at room temperature.

Another phase transition has been reported for the stoichiometric compound at about 860°C (in air) or 925°C (under pure O_2), thus passing to a simple cubic cell $Pm\bar{3}m$, with the balancing of charges $Bi^{3+} + Bi^{5+} \Leftrightarrow 2Bi^{4+}$ (7).

0022-4596/95 $6.00

The authors point out that this last structure, as well as the stoichiometry of the compound, remains unchanged up to melting (ca. 1050°C). As a matter of fact, thermogravimetric tests in air have already shown (4) that $BaBiO_3$, at temperatures higher than 650°C, loses oxygen in a reversible way, thus originating nonstoichiometric $BaBiO_{3-\delta}$ phases.

A systematic study of this phenomenon was first accomplished by Beyerlein *et al.* (8) by TG analysis on $BaBiO_3$ in flowing atmospheres with different pO_2 values (1×10^{-4} to 1 atm). Their results, which were later confirmed by Saito *et al.* (9), allowed the authors to draw out a schematic phase diagram of the whole $BaBiO_{3-\delta}$ system ($0 \leq \delta \leq 0.5$).

This diagram shows, with respect to temperature and pO_2, three distinct monophasic regions, called I, II, and III, respectively. The limits of I ($0 \leq \delta \leq 0.03$) and III ($0.42 \leq \delta \leq 0.45$) are almost constant as pO_2 changes; the limits of II, very narrow at low pO_2 values, widen progressively so much that they are mingled (for $pO_2 > 3 \times 10^{-2}$ atm) with those of I and III. In the same note (8) two other phases were pointed out, both supposed metastable, magenta- and yellow-colored, with compositions $BaBiO_{2.503}$ and $BaBiO_{2.500}$.

As already noted by Lightfoot *et al.* [10], unfortunately no X-ray diffraction (XRD) patterns were reported by Beyerlein *et al.* for most of the above phases (phase II, magenta phase, yellow phase). Only X-ray (XR) data concerning the $BaBiO_{2.55}$ phase, which belongs to zone III and has an elementary cell with tetragonal symmetry ($a = 8.754$ Å; c = 8.977 Å), are clearly reported.

Recent research carried out by XRD and/or neutron diffraction (ND) analyses at high temperatures and under controlled gaseous atmospheres (5) made it possible to ascertain that the solids of region I show the same cubic perovskitic cell as the stoichiometric $BaBiO_3$, with double-cell $Fm\bar{3}m$ type.

In regard to the solids of zone II, they have a cubic lattice with primitive cell $Pm\bar{3}m$, due to the disordered distribution of Bi^{3+} and Bi^{5+} ions in the *B* sites.

On the other hand, the real structure of the solids belonging to region III is still unknown. ND analyses at 900°C ($pO_2 = 0.01$ atm) yield a spectrogram which, based only on the strongest peaks, leads to a pseudotetragonal primitive cell ($a = 4.473$ Å, $c = 4.583$ Å) (5). The comparison between these data (recorded *in situ*) and those of Beyerlein *et al.* mentioned above (recorded at room temperature) leads to the idea that, between the various phases in the examined system, only phase III remains unchanged upon cooling.

More recently, in an olive green sample with composition $BaBiO_{2.52}$, including small amounts of $BaBiO_3$, a new phase with theoretical composition $BaBiO_{2.50}$ has been identified by Lightfoot *et al.* (10) and crystallographically characterized ($a = 7.3412$ Å, $b = 7.5793$ Å, $c = 6.0722$ Å, $\beta = 99.187°$, space group $P2_1/c$). It has still not been checked whether this new phase coincides with either of the two metastable phases (red or yellow) pointed out by Beyerlein *et al.*.

1.3. Research Aim

As already pointed out, this work will lead to a wider investigation of the BaO–Bi_2O_3–O system in air. Its first purpose is to examine the reduction isobaric curve T (°C) vs δ (for $pO_2 = 0.21$ atm) for $BaBiO_3$ up to melting, and to characterize, by XR powder diffraction, the solids produced in this process, after proper quenching from different temperatures.

With other experimental techniques we will try to find an answer to the several still unsolved questions concerning the whole $BaBiO_{3-\delta}$ system ($0 \leq \delta \leq 0.5$). The lack of reliable experimental data about the low temperature ($T < 700$°C) equilibria is indeed a first cause of uncertainty about the real pattern of the phase diagram. Not yet clearly defined is the width or even the existence of the thin diphasic I + II region for relatively high temperature and pO_2, as already emphasized by Saito *et al.* (9). Another subject worthy of attention is how the yellow and magenta phases identified by Beyerlein *et al.* (8) relate to the olive-green $BaBiO_{2.5}$ phase reported by Lightfoot (10).

2. EXPERIMENTAL

Samples of polycrystal $BaBiO_3$ were prepared by heating in air mixtures of $Ba(NO_3)_2$ and Bi_2O_3 in molar ratio 2/1. After a first heat treatment in platinum vessels at 600°C for 24 hr, the solids were carefully ground in agate mortars and further kept at 800°C for 48 hr.

This material, monophasic according to XRD analysis, was used to prepare cylindrical pellets (diameter = 10 mm; height ≈ 5 mm) to be subjected to reduction isobaric treatments in the temperature range from 750 to 1045°C. The pellets (two for each test) were placed in platinum-coated ceramic containers and introduced into tubular furnaces thermostated at different preset temperatures for every test. The heating times were 4 days at $T \leq 900°$ and about 3 days at higher temperatures. The two pellets, quenched in liquid N_2, were used to assess the δ value (by reoxidation in flowing O_2 at 600°C) and to yield XR powder diffractograms.

During quenching the duration of immersion of the pellets in liquid N_2 was controlled in order to avoid the possibility that excessive cooling might cause atmospheric moisture to condense on their surface when they were pulled out in air. As the most reduced samples were highly reactive, XRD analyses were carried out in dry and CO_2-free air.

Results of the above-described experiments led us to prepare three series of $BaBiO_{3-\delta}$ samples with δ values 0.2 (930°C), 0.3 (990°C), and 0.44 (1045°C), respectively. A fourth series, with $\delta = 0.5$, was obtained by heating $BaBiO_3$ in flowing high purity nitrogen ($O_2 \leq 1$ ppm) at 1000°C for 24 hr.

The samples of each series were used for annealing tests at different temperatures in a sheltered environment. Soon after the quenching, each pellet of a series was rolled up in thin Pt foil and sealed in an evacuated silica glass tube (ampoule internal volume, about 3 ml; specimen weight, about 4 g). The annealing cycles started for each series with a preliminary heating (24 hr) at the same temperatures as those prepared in air or N_2, and went on with step cooling (48-hr steps at constant intermediate temperatures) to 600°C. After each step one of the ampoules was quenched in water and the sample was subsequently XRD analyzed.

In order to have further data about the transition from phase I to phase II in the field of relatively high pO_2 and temperatures, simultaneous DTA, TG, and DTG tests were performed on stoichiometric $BaBiO_3$, both in air and under O_2.

3. RESULTS AND DISCUSSION

3.1. Reduction Isobar ($pO_2 = 0.21$ atm) and XRD Spectrograms of $BaBiO_{3-\delta}$ Solids ($0 \leq \delta \leq 0.44$)

The curve of T (°C) vs δ in the temperature range 750 to 1045°C (Fig. 1) shows a trend without a horizontal line, like that of $pO_2 = 0.1$ atm drawn by Beyerlein *et al.* by TG data. It can be divided into three nearly straight-line parts, with limits corresponding respectively to the temperature ranges 750 to 850°C, 850 to 1000°C, and 1000 to 1045°C.

In Fig. 2 the XRD patterns of some $BaBiO_{3-\delta}$ samples quenched in liquid N_2 at different temperatures are compared with that of stoichiometric $BaBiO_3$. They have been assembled, based on some of their distinctive features, into three groups, according to the division of the isobaric curve itself.

3.1.1. First isobar part. In Fig. 2b the spectrogram of the $BaBiO_{3-\delta}$ ($\delta = 0.035$), obtained by quenching from 840°C, has been reported as that typical of solids in the first part of the isobar. As already pointed out by other authors (7, 8, 11), these solids, which we can identify with those of region I, show practically the same diffraction pattern, i.e., that of monoclinic, fully oxidized $BaBiO_3$ (Fig. 2a). We must therefore conclude that, despite the high cooling rate, the deficient $Fm\bar{3}m$ high temperature lattice (5) undergoes the same transitions ($R\bar{3}$, $I2/m$) as the lattice of the stoichiometric $BaBiO_3$ compound. The presence of oxygen vacancies in the monoclinic lattice of these solids has been related to the appearance, on the precession photograph, of weak satellite spots besides those typical of the monoclinic lattice of the fully oxidized $BaBiO_3$ (11).

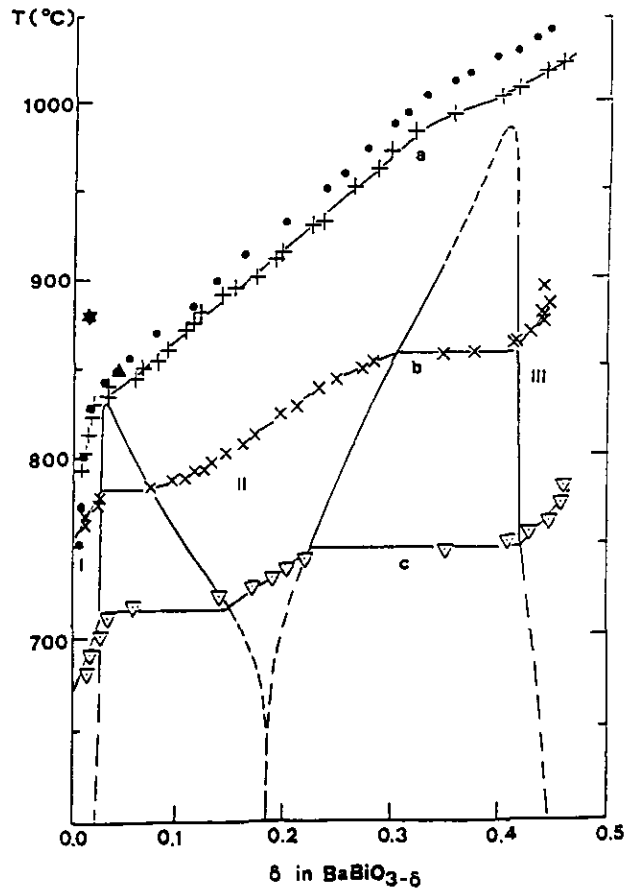

FIG. 1. $-T$ vs δ diagram of $BaBiO_{3-\delta}$ ($0 \leq \delta \leq 0.5$) (reconstructed according to (8)). (a)–(c): isobars corresponding to $pO_2 = 10^{-1}$, 10^{-2}, and 10^{-3} atm respectively (8); (●), isobar $pO_2 = 0.21$ atm (this work); transition phase I → phase II in air (▲) and in O_2 (★) by TG, DTG, and DTA simultaneous analysis.

3.1.2. Second isobar part. The solids in the second part of the isobar (850 to 1000°C) yield XRD patterns, Figs. 2c–2e, characterized by partial broadening of the monoclinic lattice lines as well as by extra peaks whose intensities progressively increase as T increases. These new peaks start to appear in the spectrograms of solid $BaBiO_{3-\delta}$ ($\delta = 0.050$) quenched from 857°C.

This pair of δ and T values agrees well with the coordinates of the apex of the biphasic I + II zone in the diagram of Fig. 1. It therefore seems reasonable to conclude that at about 850°C, in air, the transition from phase I to phase II still occurs through the biphasic region, whose width is no longer revealable by TG analysis (9). The 850°C value itself is, on the other hand, very close to that (860°C) derived from DTA data by Chaillout *et al.* (7) and wrongly suggested by these authors to be the temperature of the

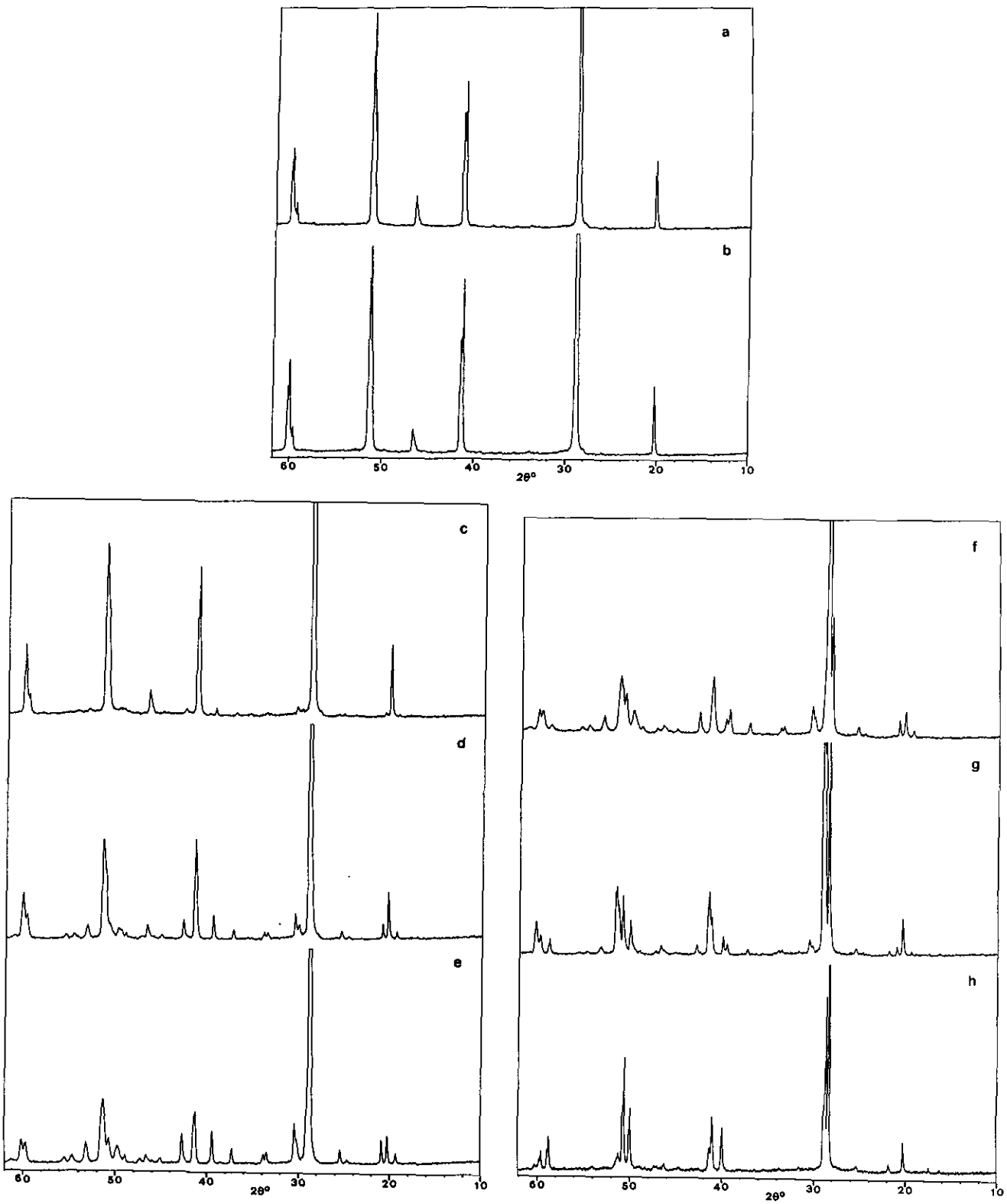

FIG. 2. Room temperature X ray powder diffraction patterns: (a) $BaBiO_3$ fully oxidated; (b) $BaBiO_{3-\delta}$ ($\delta = 0.035$) heated at 840°C in air and quenched in liquid N_2; (c) $BaBiO_{3-\delta}$ heated in air and quenched in liquid N_2 from 857°C ($\delta = 0.050$); (d) from 935°C ($\delta = 0.205$); (e) from 990°C ($\delta = 0.30$); (f) from 1015°C ($\delta = 0.33$); (g) from 1030°C ($\delta = 0.38$); (e) from 1045°C ($\delta = 0.44$).

transition from $Fm\bar{3}m$ to $Pm\bar{3}m$ for the stoichiometric compound.

As has recently been ascertained by *in situ* ND, it is a $Pm\bar{3}m$ heavily oxygen-defective lattice (5), with vacancies disorderly arranged in perovskite BiO_{6-x} octahedra, having Bi^{3+} and Bi^{4+} (7) or Bi^{3+} and Bi^{5+} (with $Bi^{3+}/Bi^{5+} > 1$) still disorderly in their centers.

The XR powder diffraction patterns reported in Figs. 2c–2e, clearly not identifiable with those of a $Pm\bar{3}m$ lattice, show that even in this case the quenching in liquid N_2 does not make it possible to freeze the high-temperature structures at room temperature. However, their distinctive features can be regarded as an indirect proof of the presence of the cubic $Pm\bar{3}m$ structure at high temperature.

The hypothesis that the extra peaks were to be ascribed to a new phase separated in the cooling (6) has not found any experimental check. As will be described at length later on, solids with different δ values, even when heat-treated in various ways, have not furnished in any case XRD patterns characterized by the sole presence of the extra peaks. On the other hand, it was not possible to ascribe some peculiar meaning to the spectrograms of solids with $\delta = 0.19$ (8), 0.21 (9), and 0.23 (11), which were suggested by the respective authors as being the real composition of phase II.

In our opinion, the quick cooling of solids of the second part of the isobaric curve, having defective $Pm\bar{3}m$ structure, still yields monophasic solids with $I2/m$-type structure heavily troubled by the presence of oxygen vacancies forcedly ordered in preferential sites, thus justifying the additional reflections besides the broadened ones of the monoclinic lattice.

3.1.3. Third isobar part. The solids related to the last part of our isobar (1000 to 1045°C) show a good tendency to sintering and crystal growth; samples heated at 1045°C for 3 days and quenched in liquid N_2 yielded aggregates of large single bright black crystals (up to 3 mm in size). The XR powder diffractograms of these solids seem still more complex, due to the appearance of new reflections, Figs. 2f–2h. Their intensities progressively increase at increasing temperatures, whereas those coming from the above-described transformations of the $Pm\bar{3}m$ cubic phase progressively weaken. These last peaks are still evident in the spectrogram of a solid quenched from 1045°C ($\delta = 0.44$), as shown in Fig. 2h.

The d values of the highest peaks of this last spectrogram agree with those taken by Beyerlein *et al.* for samples of phase III with composition $BaBiO_{2.55}$. Moreover, the pattern of this XR diffractogram coincides with that obtained by ND *in situ* (at 900°C and $pO_2 = 0.01$ atm) by Pei *et al.* (5) from specimens of phase III.

Data from solids belonging to the last part of the isobaric curve indicate that the phase II to III transition is gradual along the 1000 to 1045°C segment of our isobar. This phenomenon was already pointed out by Pei *et al.* (5) by *in situ* experiments in the temperature range from 830 to 880°C (with $pO_2 = 0.01$ atm).

It is difficult to explain this if we suppose that in the examined transition the Ba/Bi atomic ratio remains strictly unchanged. We observed an analogy between the spectrograms of solids of region III and those of terms of the Aurivillius (12) series $Bi_{2-x}Ba_{2x}O_{3-x}$ ($0.2 \leq x \leq 0.5$) with tetragonal symmetry, characterized by attenuation or full extinction of $h + k + l = 2n + 1$ reflections. This could suggest a new hypothesis about the thermodynamic and structural aspects of the II to III phase transition. We think that this transformation could proceed just through a reciprocal partial substitution of Ba and Bi ions in A and B sites, giving rise to anomalous perovskitic structures like $BaBi_3O_{5.5}$ ($x = 0.25$) (1) and $BaBi_2O_4$ ($x = 0.33$) (12). Phase III would thus become the limit term ($x = 0.5$) of this series, stable at high temperature.[1]

The reliability of our assumption is proved by comparing the XRD patterns of the terms with $x = 0.45$, 0.48, and 0.5 ($BaBiO_{2.56}$) obtained by reheating them in air at 950, 1000, and 1045°C, respectively, and quenching in liquid N_2 (Fig. 3).

3.2. Treatments of $BaBiO_3$ in Flowing N_2 and Annealing of $BaBiO_{2.50}$ in Silica Glass Ampoules

The $BaBiO_3$ compound, when heated at 1000°C for 24 hr in flowing high purity N_2 and quenched in liquid N_2, yielded a wine-red solid, with composition $BaBiO_{2.50}$. The XRD pattern (Fig. 4a), typical of solids belonging to region III, made it possible to ascertain that the above monophasic field extends, at 1000°C, as far as the $\delta = 0.5$ limit. The variable color (from black to red) of this phase can be related to oxygen content ranging from $\delta = 0.45$ to 0.5.

Reductions carried out at temperatures in the range 1000 to 800°C still yielded bright red solids with composition $BaBiO_{2.50}$. The XRD pattern of Fig. 4b, taken on a sample quenched from 900°C, appears completely different from the preceding one, but its results are nevertheless still similar to that of solids having pseudocubic perovskite structure. It is likely that the solids we obtained in this temperature range can be identified with the "magenta" phase pointed out by Beyerlein *et al.* (8). The numerous peaks instead of the single ones typical of a cubic lattice with primitive cell, together with other weak reflections, lead us to hypothesize a structure more complex than that proposed by the above authors for these solids.

The reduction rate for $BaBiO_3$ in flowing nitrogen at

[1] As already mentioned in the introduction, preliminary investigations of $Bi_{2-2x}Ba_{2x}O_{3-x}$ solids ($0.25 \leq x \leq 0.5$) of low temperature showed the biphasic nature of these solids, due to the presence of monoclinic $BaBiO_3$ in addition to the cubic form of $BaBi_3O_{5.5}$ (1).

FIG. 3. Room temperature X ray powder diffraction patterns of some terms of the Aurivillius series $Bi_{2-2x}Ba_{2x}O_{3-x-\delta}$ heated in air and quenched in N_2: (a) $x = 0.45$, from 950°C; (b) $x = 0.48$, from 1000°C; (c) $x = 0.50$, from 1045°C.

$T < 800$°C is very low. Pellets treated at 750°C for 48 hr gave heterogeneous color results from pale yellow on the surface to green and finally black in the inner zone. At this temperature two other heat treatments were necessary, with intermediate grinding and pelleting, in order to finally obtain a yellow solid with formula $BaBiO_{2.50}$, characterized by the XRD pattern shown in Fig. 4c.

The low-temperature form ($T = 800$°C) obtained in this way showed a bright yellow colour like that of the phase with the same composition described by Beyerlein *et al.* The XRD pattern of this phase is identical with that we obtained by directed reduction of $BaBiO_3$ in flowing N_2 at 750°C. It is readily indexable (see Table 1) on the basis of the crystallographic data reported by Lightfoot *et al.* (10) for the above-quoted $BaBiO_{2.50}$ phase with monoclinic symmetry.

3.3. Heat Treatments of $BaBiO_{3-\delta}$ ($\delta = 0.2, 0.3,$ and 0.44) in Silica Glass Ampoules

The results of annealing solids with $\delta = 0.2$, 0.3, and 0.44 in the way previously described were especially helpful for understanding the phase equilibria in the examined system in the low-temperature region ($T < 700$°C), until now not experimentally verified.

In the annealing tests at $T \geq 700$°C the progress of the examined solids was as a whole in good agreement with the diagram scheme proposed by Beyerlein *et al.* (Fig. 1). The monophasic solids with $\delta = 0.2$ (region II) and 0.44 (region III), annealed for at least 3 days at 900, 800, and 700°C, yielded indeed XRD patterns like those of the same samples before heat treatment (Figs. 5a, 5b and 7a, 7b).

Still the behavior of the $\delta = 0.3$ solid, which belongs to region II at 1000°C, agrees with the above diagram scheme after annealing at 900, 800, and 700°C, and provides XR patterns typical of biphasic solids (II + III) with progressively increasing amounts of phase III (Figs. 6a, 6b).

The spectrograms of Figs. 5c, 6c, and 7c, taken on the solids annealed at 600°C, show that at this temperature, contrary to what has been proposed by Beyerlein *et al.* (8) and Saito *et al.* (9), both phases II and III are thermodynamically unstable, due to their decomposition in physical mixtures of phase I and the yellow $BaBiO_{2.50}$ phase.

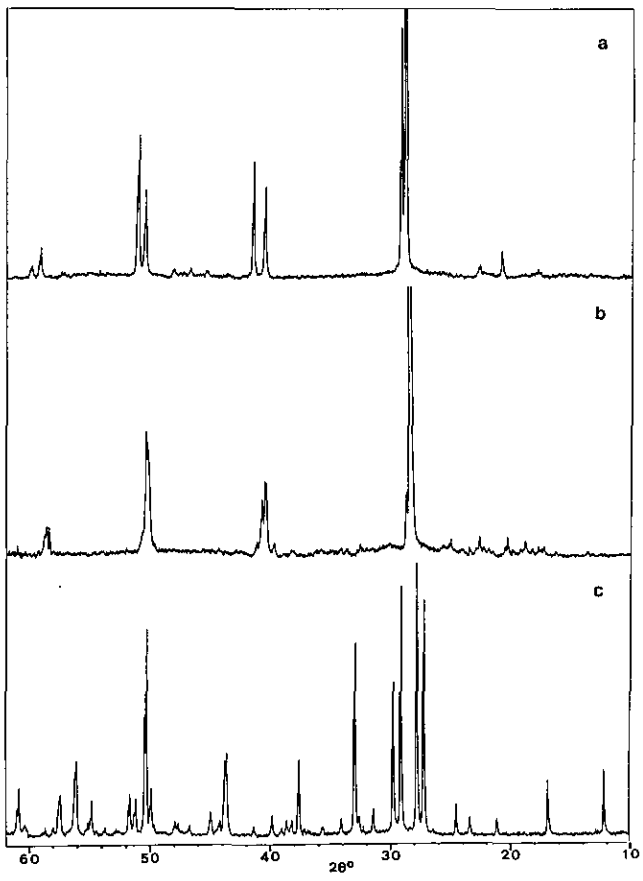

FIG. 4. Room temperature X ray powder diffraction patterns of the different $BaBiO_{2.50}$ modifications obtained by reduction of the $BaBiO_3$ in high-purity N_2 and quenching in liquid N_2: (a) from 1000°C = tetragonal form (phase III); (b) from 950°C = pseudocubic form (magenta phase); (c) from 750°C = monoclinic phase (yellow phase).

TABLE 1

Theta	*hkl*	Int.cal	Theta	*hkl*	Int.cal
6.117	100	138.3	21.894	$\bar{2}12$	228.5
8.463	$1\bar{1}0$	129	22.121	$\bar{3}02$–311	33
10.557	$\bar{1}11$	84.6	22.503	$\bar{3}21$	56.1
11.705	020	108	23.397	$\bar{1}13$	46.2
12.231	200	29.4	23.850	231	48
13.639	210	385	23.993	040	110.5
13.918	$0\bar{2}1$	837.5	24.850	$1\bar{4}0$	20
14.583	$\bar{2}11$	1003.7	24.983	$\bar{2}13$	197.2
14.913	002	811.6	25.192	$\bar{4}00$	177.6
15.740	$12\bar{1}$	154	25.628	$\bar{2}32$	240
16.333	$\bar{1}12$	74.6	25.872	023	117
16.516	211	853.6	26.400	$14\bar{1}$	7.5
17.083	$10\bar{2}$	69.4	26.880	$3\bar{1}2$	36.7
17.879	$\bar{2}02$–$\bar{2}21$	37.4	27.220	$\bar{2}23$	14.5
18.835	$\bar{2}12$	398.3	27.442	$\bar{4}02$	133
19.139	$02\bar{2}$	37.7	27.600	$12\bar{3}$	61.7
19.380	$\bar{1}22$	54	28.090	$\bar{3}13$–$\bar{4}21$	400
19.566	$3\bar{1}0$	12.8	28.767	213–042	200
19.948	$\bar{3}11$–$\bar{1}31$	127.9	29.04	$3\bar{2}2$	10.9
20.724	131	56.5	29.351	$\bar{1}33$	36.9
21.820	230	264.4			

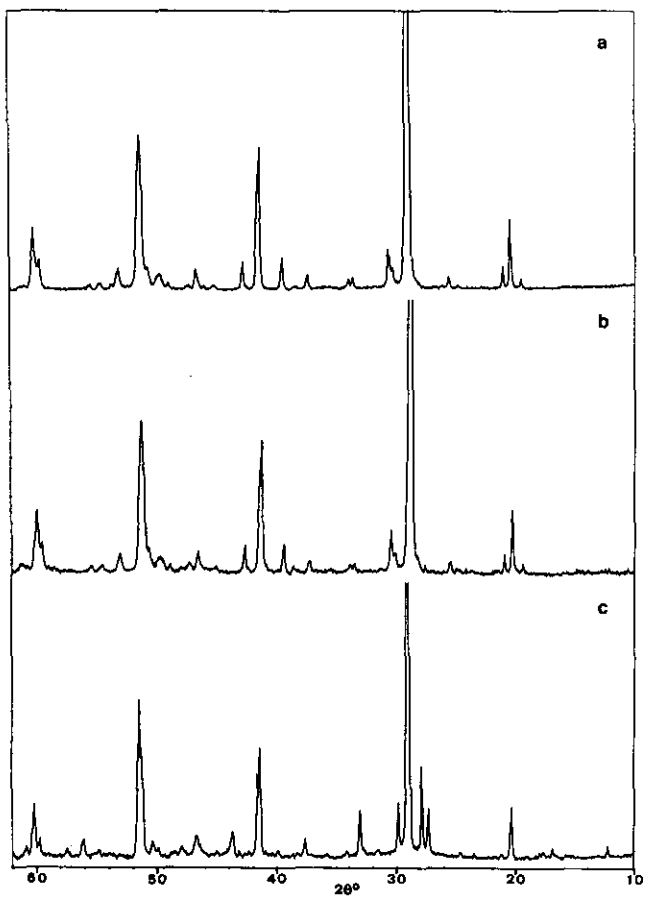

FIG. 5. Room temperature X ray powder diffraction patterns of $BaBiO_{3-\delta}$ ($\delta = 0.2$) annealed in silica glass tubes: (a) at 900°C; (b) at 700°C; (c) at 650°C.

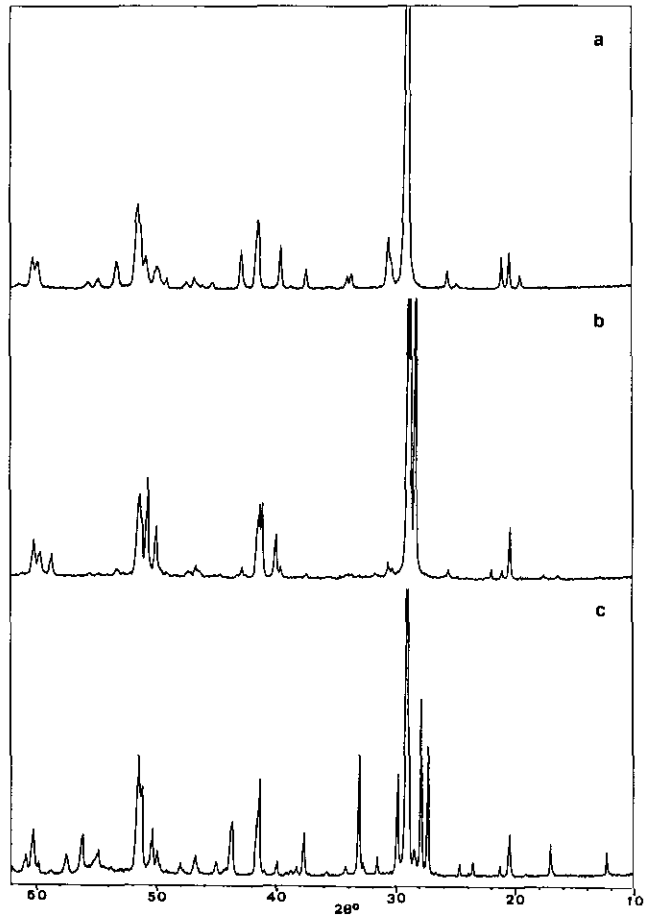

FIG. 6. Room temperature X ray powder diffraction patterns of $BaBiO_{3-\delta}$ ($\delta = 0.3$) annealed in silica glass tubes: (a) at 900°C; (b) at 700°C; (c) at 650°C.

Careful investigation in the range from 700 and 650°C made it possible to narrow the temperature range in which both phases decompose to 670–660°C. Even considering the precision limits of the experimental technique employed, further tests in this narrow range made it possible to assess the equilibria:

(a) phase II $\Leftrightarrow$ phase I + phase III (668 ± 2°C)

(b) phase III $\Leftrightarrow$ phase I + yellow phase (663 ± 2°C).

In light of these results, especially for the first equilibrium, the value $\delta \approx 0.20$ (0.19 (8) and 0.21 (9)) assumes now the meaning of the eutectoid composition of phase II in invariant equilibrium with phases I and III.

3.4. Simultaneous DTA, TG, and DTG Tests on $BaBiO_3$ in both Dry CO_2-Free Air and Flowing O_2

The results of the DTA, TG, and DTG simultaneous tests on the stoichiometric $BaBiO_3$, with $pO_2 = 0.21$ and 1 atm, are reported in Fig. 8. The DTA curves show for both tests sharp endothermic peaks upon heating, with a maximum at 847°C in air or at 880°C in O_2. This test is thus experimental evidence of the assumption of Saito *et*

FIG. 7. Room temperature X ray diffraction patterns of $BaBiO_{3-\delta}$ ($\delta = 0.44$) annealed in silica glass tubes: (a) at 900°C; (b) at 700°C; (c) at 650°C.

al. (9) that these thermal anomalies are to be still assigned to the I to II phase transition, no longer detectable by TG analysis alone.

As a matter of fact, the DTG curves show that the DTA endothermic signals are joined to $-dm/dT$ vs T peaks originating from quick lowering of the oxygen content when the examined solids pass through the biphasic region I + II.

The comparison between the intensities of the DTA and DTG signals registered in air or in O_2 shows that the change of oxygen content in the I to II phase transition progressively weakens as the pO_2 of the gaseous phase increases. This justifies the observation of Saito *et al.* (9) that the biphasic region I + II narrows more and more as temperature and pO_2 increase. The δ value, as estimated from the total weight loss measured at 847 ($\delta = 0.05$) and 880°C ($\delta = 0.015$), allowed us to precisely draw the trend, in the T vs δ diagram, of the narrow transition zone we are considering.

The two pairs of values (T, δ) reported above are nearly aligned with the curve limit of the monophasic region I (Fig. 1). This leads us to think that, at appropriate oxygen pressures ($pO_2 > 1$ atm), the width of the biphasic zone I + II has to come to a point, with coordinates $\delta = 0$ and T = temperature of the $Fm\bar{3}m$ to $Pm\bar{3}m$ transition of stoichiometric $BaBiO_3$. This also means that under suitable experimental conditions ($pO_2 > 1$ atm; $T > 880$°C) the limit of region II coincides with the stoichiometric $BaBiO_3$ itself, with primitve cell $Pm\bar{3}m$.

4. CONCLUSIONS

(a) Heat-treatments in air of the compound $BaBiO_3$ lead to nonstoichiometric $BaBiO_{3-\delta}$ phases and, at 1045°C (close to the melting temperature), the solid assumes the composition $BaBiO_{2.56}$.

The T vs. δ curve (750 to 1045°C) shows three near-linear sections between 750 and 850°C, 850 and 1000°C, and 1000 and 1045°C.

The $Fm\bar{3}m$ perovskitic cubic structure of solids of the first section of the isobar (region I of Beyerlein *et al.*, Fig. 1) undergoes, during the quenching in liquid N_2, the same transformations as the stoichiometric compound and the XRD patterns at room temperature do not differ from that of the monoclinic $BaBiO_3$.

Even the $Pm\bar{3}m$ structure of the solids of the second part of the isobaric curve (region II) undergoes analogous transformations during quenching. In this case, however, due to the high vacancy concentration, a monoclinic struc-

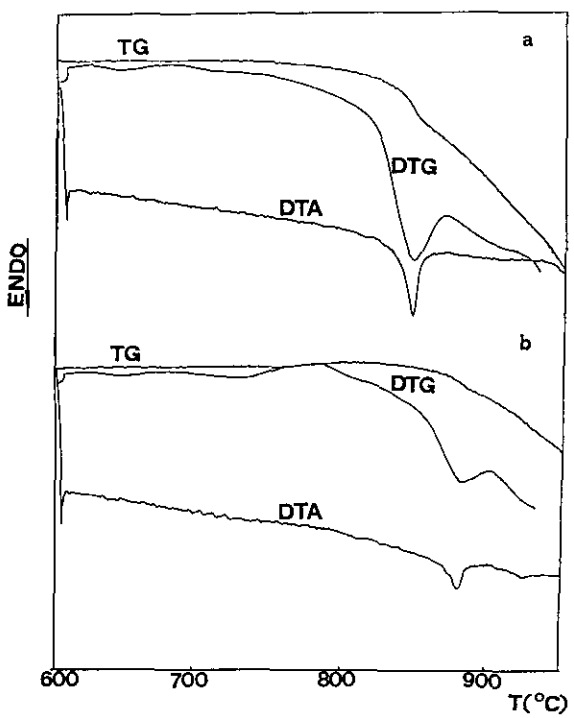

FIG. 8. TG, DTG, and DTA curves at a heating rate of 5°C/min: (a) in air; (b) in O_2.

ture is achieved, largely metastable with oxygen vacancies forcedly ordered in preferential sites.

As already pointed out by Pei *et al.* in their *in situ* diffraction experiments, the phase II to phase III transition occurs gradually and involves the whole temperature range corresponding to the last part of the isobar.

The close resemblance between the XR spectrogram of the solid $BaBiO_{2.56}$ (phase III) and those of the richest Ba terms of the Aurivillius series $Bi_{2-2x}Ba_{2x}O_{3-x+\delta}$ ($0.25 \leq x \leq 0.5$) leads us to think that in the examined transition, the Ba and Bi ions themselves, at first distinct in their respective *A* and *B* sites, are involved in an order to disorder transformation.

(b) The heating of $BaBiO_3$ in high purity N_2 yields the polymorphous solid $BaBiO_{2.50}$. The low temperature ($T \leq 800$°C), bright yellow form shows a XRD pattern readily interpretable on the basis of the crystallographic data of the olive-green monoclinic phase identified by Lightfoot *et al.* (10), with nominal formula $BaBiO_{2.50}$.

For temperatures in the range 800 to 1000°C the solid $BaBiO_{2.5}$ shows a bright red color (probably coinciding with the magenta phase of Beyerlein *et al.*) and its XRD spectrogram is like that of a pseudocubic perovskite.

The examined solid, when quenched from 1000°C, shows on the contrary, a wine-red color and its XRD pattern is identifiable with that typical of tetragonal phase III.

(c) Annealings of $BaBiO_{3-\delta}$ solids (with $\delta = 0.2$, 0.3, and 0.44) sealed in silica glass tubes, clearly showed that for $T \leq 660$°C the system $BaBiO_{3-\delta}$ is characterized by the coexistence of the yellow phase ($BaBiO_{2.5}$) and phase I ($BaBiO_3$).

This condition is reached, during cooling, through two distinct invariant equilibria:

(a) phase II ($\delta = 0.2$) $\Leftrightarrow$ phase I + phase III
$T = 668$°C

(b) phase III $\Leftrightarrow$ phase I + yellow phase
$T = 663$°C.

(d) The results of simultaneous TG, DTG, and DTA tests concerning the phase I to phase II transition, in the region of comparatively high temperatures and pO_2 values, provided precise information about the trend of the state diagram in the richest oxygen zone of the $BaBiO_{3-\delta}$ system. These results lead us to predict the existence of a temperature $T_{(\delta=0)}$ for the transition from $Fm\bar{3}m$ to $Pm\bar{3}m$ of the stoichiometric compound $BaBiO_3$ when heated at oxygen pressures suitable to preserve its stoichiometry ($pO_2 > 1$ atm). At temperatures higher than the transition one, $T_{(\delta=0)}$, the stoichiometric compound appears therefore to be the limit term of monophasic region II with a $Pm\bar{3}m$ defective lattice.

(e) The two lattices $Fm\bar{3}m$ and $Pm\bar{3}m$ have different abilities for accomodating oxygen vacancies, and it is well known that $SrTiO_{3-\delta}$ (with $Pm\bar{3}m$ structure) is thermodynamically stable in the whole $\delta = 0$–0.5 range. This justifies the strong difference in width between monophasic regions I and II and the trend of the phase diagram itself.

As occurs in other already known systems formally similar to that examined (i.e., Fe–Fe_3C, characterized by the transition from bcc-Fe to fcc-Fe), the presence of oxygen vacancies in $BaBiO_{3-\delta}$ solids make the $Pm\bar{3}m$ structure thermodynamically stable at temperatures lower than that of transition $T_{(\delta=0)}$ of the stoichiometric compound.

The eutectoid temperature (about 668°C) at which the monophasic field of the defective $Pm\bar{3}m$ comes to a point ($\delta = 0.2$) corresponds to the minimum value beyond which the examined phase gives thermodynamically unstable results.

The eutectoid transformation phase II ($\delta = 0.2$) $\Leftrightarrow$ phase I + phase III occurs through a slow process of nucleation and growth of crystals of the phase less rich in oxygen (phase III) and simultaneous transition from $Pm\bar{3}m$ to $Fm\bar{3}m$ of the lattice of the remaining solid free of oxygen vacancies.

A high cooling rate hinders the nucleation of phase III, without suppressing the sequence of transitions from $Pm\bar{3}m$ to $I2/m$ (monoclinic), thus giving rise to strongly metastable structures with oxygen vacancy concentrations larger than the $I2/m$ lattice can accommodate.

ACKNOWLEDGMENT

The authors gratefully acknowledge Professor C. Brisi for his helpful discussions.

REFERENCES

1. F. Abbattista, M. Hervieu, M. Vallino, C. Michel, and B. Raveau, *J. Solid State Chem.* **104,** 338 (1993).
2. V. V. Saponov, P. Kostic, I. Krstanovic, and M. M. Ristic, *Silic. Ind.* **5,** 165 (1990).
3. D. E. Cox and A. W. Sleight, *Solid State Commun.* **19,** 969 (1976).
4. D. E. Cox and A. W. Sleight, *Acta Crystallogr. Sect. B* **35,** 1 (1979).
5. S. Pei, J. D. Jorgensen, D. G. Hinks, P. Lightfoot, Y. Zheng, D. R. Richards, B. Dabrowski, and A. W. Mitchell, *Mater. Res. Bull.* **25,** 1467 (1990).
6. H. Kusuhara, A. Yamanaka, H. Sakuma, and H. Hashizume, *Jpn. J. Appl. Phys.* **28,** 678 (1989).
7. C. Chaillout, A. Santoro, J. P. Rameika, A. S. Cooper, G. P. Espinosa, and M. Marezio, *Solid State Commun.* **65,** 1363 (1988).
8. R. A. Beyerlein, A. J. Jacobson, and L. N. Yacullo, *Mater. Res. Bull.* **20,** 877 (1985).
9. Y. Saito, T. Maruyama, and A. Yamanaka, *Thermochim. Acta* **115,** 199 (1987).
10. P. Lightfoot, J. A. Hriljac, S. Pei, Y. Zheng, A. W. Mitchell, D. R. Richards, B. Dabrowski, J. D. Jorgensen, and D. G. Hinks, *J. Solid State Chem.* **92,** 473 (1991).
11. C. Chaillout and J. P. Rameika, *Solid State Commun.* **56,** 833 (1985).
12. B. Aurivillius, *Ark. Kemi Mineral. Geol.* **16A,** 1 (1943).
13. R. Arpe and H. Müller-Buschbaum, *Z. Anorg. Allg. Chem.*, **434,** 73 (1977).